7. Iqbal, Z., and E. Weidekamm. 1980. Raman and infrared spectroscopic study of gramicidin A conformations. *Arch. Biochem. Biophys.* 202:639–649.
8. Lotz, B., F. Colonna-Cesari, F. Heitz, and G. Spach. 1976. A family of double helices of alternating poly(γ-benzyl-D-L-glutamate), a stereochemical model for gramicidin A. *J. Mol. Biol.* 106:915–942.
9. Nabedryk, E., M. G. Gingold, and J. Breton. 1982. Orientation of gramicidin A transmembrane channel. Infrared dichroism study of gramicidin in vesicles. *Biophys. J.* 38:243–249.
10. Urry, D. W., R. G. Shaw, T. L. Trapane, and K. U. Prasad. 1983. Infrared spectra of the gramicidin A transmembrane channel: the single stranded β^6-helix. *Biochem. Biophy. Res. Commun.* 114:373–379.

ACTIVATION AND INACTIVATION OF MELITTIN CHANNELS

M. T. TOSTESON AND D. C. TOSTESON
Department of Physiology and Biophysics, Harvard Medical School, Boston, Masachusetts 02115

Melittin, the major toxin of the bee venom, produces a variety of effects on natural membranes, including cell lysis, activation of phospholipase A, antimicrobial activity and alterations in mitochondrial respiration and adenylate cyclase activity (1). We have recently shown that this amphiphilic peptide, which consists of 26 amino acid residues, including six with positively charged side chains, induces a voltage-dependent conductance in lecithin (asolectin) bilayers (2). The present communication describes in detail the temporal course of this conductance induced by melittin.

MATERALS AND METHODS

All salts used were reagent grade. Melittin was either purchased from Sigma Chemical Co. (St. Louis, MO) or kindly provided by Dr. S. C. Quay. Bilayers were made from asolectin (Associated Concentrates, Long Island, NY) by apposition of two monolayers (3). The area of the films ranged from 0.05×10^{-2} to 1.3×10^{-2} cm^2. The aqueous solutions contained unbuffered 1 M NaCl. Melittin was added to one aqueous compartment (*cis*) as small aliquots of a concentrated ethanolic solution. The final ethanol concentration was always less than 1%.

Currents were measured using a fast-settling, high input impedance amplifier (LF157A, National Semiconductors), DC pulses of varying amplitude and duration were applied using a programmable function generator (model 5900, Krohn-Hite Co., Avon, MA). The sign of the potential refers to the compartment to which melittin was added. Positive charge flowing from the *cis* to the *trans* compartment is plotted as positive (upward) current.

RESULTS AND DISCUSSION

Fig. 1 *A* shows the temporal course of the current across an asolectin bilayer in response to a step in voltage. The first fast rise in current (*a*) is depicted with better time resolution in panel 1 *B*, where it is seen that this first current increase shows activation that reaches a steady-state ($dI/dt = 0$) with a half-time of 0.5 to 2 ms. The current-voltage (*I-V*) curve of the steady-state current, shown in Fig. 2 *A*, yields the (lg *G*)-*V* curve shown in 2 *B*. From these curves it is possible to calculate that the conductance changes *e*-fold/16–20 mV change in the applied potential. Also

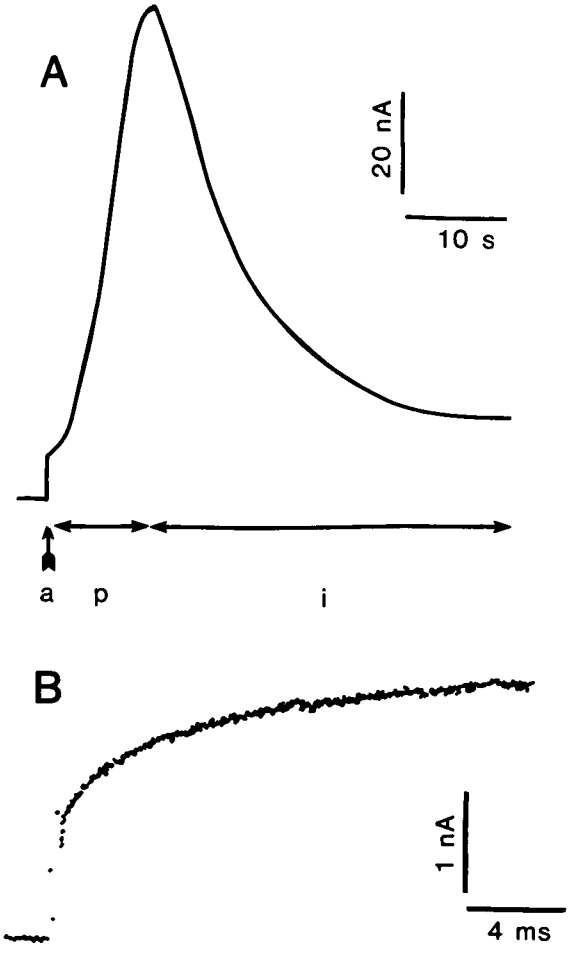

FIGURE 1 Time course of the current response to a constant voltage pulse. *A*, current response to a step in voltage. The +62 mV pulse was started at the arrow and was maintained through the region labeled *i*. *B*, current response to a step in voltage of short duration. 30 pulses of 20 ms duration and +62 mV amplitude were applied to the bilayer with a frequency of 10 Hz before the sequence shown in panel *A* was obtained. The individual current responses were added in a signal averager, after compensation for the bilayer capacitance. Melittin concentration (*cis*-side only): 1.5×10^{-7} M.

BIOPHYS. J. © Biophysical Society · 0006-3495/84/01/112/03 $1.00
Volume 45 January 1984 112–114

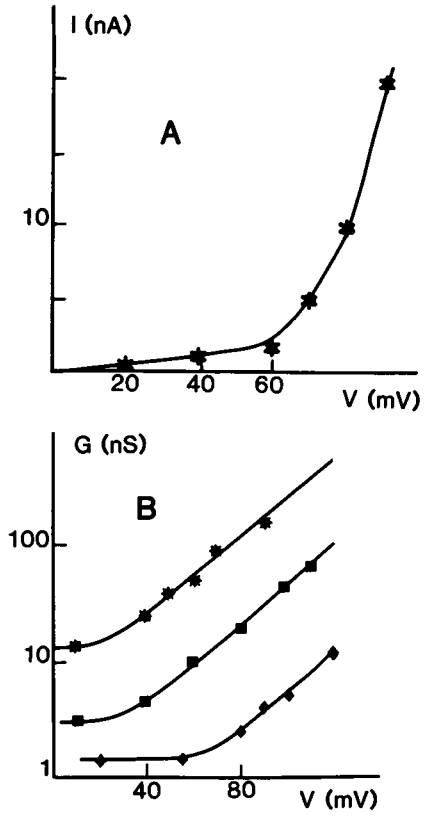

FIGURE 2 Voltage-dependence of the steady-state conductance of region *a*. *A*, current vs. voltage (*I-V*) curve obtained with 1.5×10^{-7} M melittin on *cis*-side. The current at each potential was measured using repetitive pulses as explained in Fig. 1 *B*. *B*, steady-state conductance (*G*, logarithmic scale) vs. voltage, obtained in the presence of increasing concentration of melittin added to the *cis*-side of a lipid bilayer. After each addition of an aliquot of a concentrated solution of melittin, the current response to +80 mV (I_{80}) was tested every 10–15 min, using the pulse sequence as in Fig. 1 *B*. When I_{80} reached a constant, reproducible value, a complete *IV* curve was obtained. Reproducible (lg *G*)-*V* curves were generally obtained 30–45 min after addition of melittin. Melittin concentrations: 0.75×10^{-7} M; 1.0×10^{-7} M; 1.5×10^{-7} M.

shown, in 2 *B*, is the fact that varying the aqueous melittin concentration results in (1g *G*)-*V* curves that are parallel, indicating that the dependence of the conductance on voltage does not change as the aqueous peptide concentration is changed. At a fixed voltage, the magnitude of the conductance increases as the fourth power of the increase in the melittin concentration. Thus, the first region of the conductance activation, *a*, seems to involve a tetramer of melittin. Furthermore, the opening of this conductive pathway seems to be associated with the movement of the equivalent of one electronic charge across the electric field of the bilayer.

After the activation of (*a*) is completed, the current continues to rise along an S-shaped curve and reaches a new steady-state (cf. Fig. 1, region *p*). The steady-state conductance in this region increases *e*-fold/6-mV increase in the voltage, and at a fixed voltage, it increases as the fourth power of the melittin concentration (2). Thus, the opening of each conductance pathway in region *p* involves the displacement of four equivalent electronic charges by the electric field across the bilayer. We speculate that the slow activation of the conductance (region *p*) involves the formation of a different tetramer from that responsible for the conductance observed in region *a*.

Fig. 3 illustrates the strategy and the results of experiments conducted to study the time course of closing of the conducting units which are open during the steady-state *p*. After allowing the conductance to reach steady-state *p* at V_2, the membrane voltage was changed to V_3 (in this case, −10 mV). At intervals, test pulses of 15-ms duration at V_2 were applied to the membrane. The current in response to the test pulse decreases as two exponential functions of the time the potential remains at V_3 (cf. Fig. 3). The time constant for the fastest of the two processes is 50 ms.

When V_2 is maintained beyond region *p*, the conductance declines (inactivation) and eventually reaches a new steady-state (cf. Fig. 1, region *i*). The rate of inactivation was found to be voltage-dependent, changing *e*-fold for every 9-mV change in the voltage (Fig. 4 *A*). The extent of

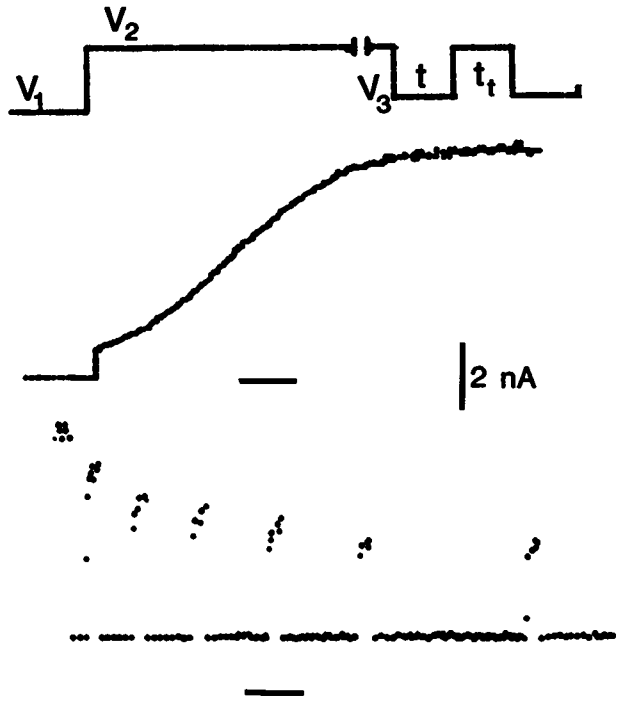

FIGURE 3 Kinetics of closing of the conductance pathway. *top*, Pulse sequence used to measure the rate of closing of the conductance pathway. After the bilayer current reached steady-state (*middle curve*) in response to a step in voltage from V_1 to V_2, the membrane potential was changed to V_3. At intervals of time *t*, test pulses (to V_2) of duration t_t were applied and the current response recorded. *bottom*, Current sequence corresponding to the first six responses in the sequence of nine test pulses. $V_1 = -10$ mV; $V_2 = +54$ mV; $V_3 = -10$ mV; $t_t = 15$ ms. Test pulses were applied using the following sequence for *t*, the time the potential remained at V_3: 15, 30, 45, 60, 75, 150, 750, 1,500, and 7,500 ms. Time scale: 3 s for middle curve, 75 ms for bottom curve. Melittin concentration (*cis*-side only): 1.25×10^{-7} M.

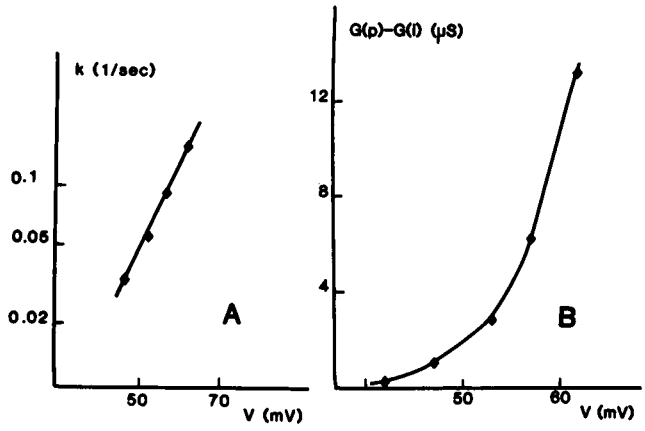

FIGURE 4 Characteristics of the inactivation of the conductance. *A*, rate of inactivation (k, log scale) vs. potential. k was calculated from plots of the log conductance vs. time for the data of the region labeled *i* in Fig. 1 *A*. *B*, voltage dependence of the extent of inactivation as determined from the difference between the steady-state conductance of region *p* (G_p) and the steady-state conductance of region *i* (G_i). Melittin concentration (*cis*-side only): 1.0×10^{-7} M.

inactivation, $(G_p - G_i)$ is also voltage dependent, as illustrated in Fig. 4 *B*.

In summary, the time course of the melittin-induced conductance in bilayers shows two distinct steady-state regions which differ both in the kinetics of activation and in their voltage dependence. One region, *a*, activates rapidly in response to changes in V (time constants of 1–2 ms) and has a gating charge = 1. The other region, *p*, activates more slowly (time constants of 2–10 s) and has a gating charge = 4. The magnitude of the steady-state conductance (at a fixed voltage) in both regions is proportional to the fourth power of the concentration of melittin monomers in the aqueous solution.

Elucidation of the difference in the molecular arrangements responsible for these two regions should shed light on how polymers of L-amino acids can induce ionic conductances in lipid bilayers and, possibly, in biological membranes.

This work was supported by grant GM-25277 from the National Institutes of Health.

Received for publication 12 May 1983.

REFERENCES

1. Habermann, E. 1972. Bee and wasp venoms. *Science (Wash., DC)*. 177:314–322.
2. Tosteson, M. T., and D. C. Tosteson. 1981. The sting. Melittin forms channels in lipid bilayers. *Biophys. J.* 36:109–116.
3. Montal, M., and P. Mueller. 1972. Formation of bimolecular membranes from lipid monolayers and a study of their electrical properties. *Proc. Natl. Acad. Sci. USA.* 69:3561–3566.

ION-BOUND FORMS OF THE GRAMICIDIN A TRANSMEMBRANE CHANNEL

B. A. WALLACE
Department of Biochemistry, Columbia University, New York, New York 10032

The physical characteristics and conductance properties of gramicidin A, a linear polypeptide antibiotic that forms transmembrane ion channels, have been extensively investigated. The molecule adopts distinctly different conformations in membranes and in organic solvents (1). The membrane-bound form is an amino-terminus-to-amino-terminus helical dimer (2), whereas in organic solvents the molecule appears to form a series of parallel and antiparallel interwined double helices (3), (Fig. 1). The circular dichroism (CD) spectrum of gramicidin in methanol solution is easily distinguishable from that of gramicidin bound to vesicles either by cosolubilization (4) or by heat treatment (5), although both methods of vesicle incorporation produce similar results.

Because gramicidin specifically binds monovalent cations (6, 7), it was of interest to examine the effects of ion binding on the various conformations of the molecule and to determine the relationship of the ion-bound forms to the channel structure. Binding of Cs^+ to the membrane-bound form results in no change in the peptide backbone conformation (4), whereas binding to the methanol solution structures produces not only a change in pitch of the helix, but also a net change in handedness of at least the predominant form of double-helix dimer (8, 1). None of the conformations in methanol (either with or without Cs^+) resembles the membrane-bound form. Even when gramicidin is loaded with Cs^+ in a methanol solution prior to binding to vesicles, the spectrum of the incorporated

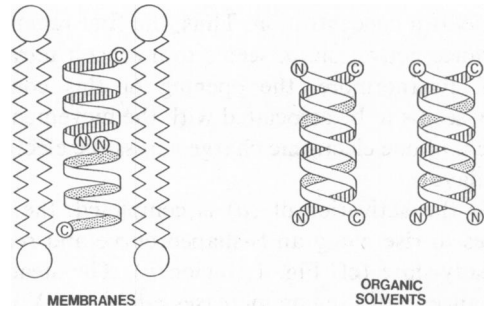

FIGURE 1 Schematic diagram of the conformations of gramicidin A in phospholipid bilayers and in organic solvents.

BIOPHYS. J. © Biophysical Society · 0006-3495/84/01/114/03 $1.00
Volume 45 January 1984 114–116